Measurement Report: Ammonia in Paris derived from ground-based open-path and satellite observations

Camille Viatte[1], Nadir Guendouz[1], Clarisse Dufaux[1], Arjan Hensen[2], Daan Swart[3], Martin Van Damme[4,5], Lieven Clarisse[4], Pierre Coheur[4], and Cathy Clerbaux[1,4]

[1]LATMOS/IPSL, Sorbonne Université, UVSQ, CNRS, Paris, France;

[2]Netherlands Organisation for Applied Scientific Research (TNO), P.O. Box 15, 1755 ZG, Petten, the Netherlands

[3]National Institute for Public Health and the Environment (RIVM), Bilthoven, the Netherlands;

[4]Université libre de Bruxelles (ULB), Spectroscopy, Quantum Chemistry and Atmospheric Remote Sensing (SQUARES), Brussels, Belgium;

[5]BIRA-IASB - Belgian Institute for Space Aeronomy, Brussels, Belgium;

Correspondence: Camille Viatte (camille.viatte@latmos.ipsl.fr)

Abstract

Ammonia (NH_3) is an important air pollutant which, as precursor of fine particulate matter, raises public health issues. This study analyzes 2.5-years of NH_3 observations derived from ground-based (miniDOAS) and satellite (IASI) remote sensing instruments to quantify, for the first time, temporal variabilities (from interannual to diurnal) of NH_3 concentrations in Paris.

The IASI and miniDOAS datasets are found to be in relatively good agreement (R>0.70) when atmospheric NH_3 concentrations are high and driven by regional agricultural activities. Over the investigated period (January 2020 – June 2022), NH_3 average concentrations in Paris measured by the miniDOAS and IASI are 2.23 µg.m^{-3} and 7.10x10^{15} molecules.cm^{-2}, respectively, which are lower or equivalent to those documented in other urban areas. The seasonal and monthly variabilities of NH_3 concentrations in Paris are driven by sporadic agricultural emissions influenced by meteorological conditions, with NH_3 concentrations in spring up to 2 times higher than in other seasons.

The potential source contribution function (PSCF) reveals that the close (100-200km) east and northeast regions of Paris constitute the most important potential emission source areas of NH_3 in the megacity.

Weekly cycles of NH_3 derived from satellite and ground-based observations show different ammonia sources in Paris. In spring, agriculture has a major influence on ammonia concentrations and, in the other seasons, multi-platform observations suggest that ammonia is also controlled by traffic-related emissions.

In Paris, the diurnal cycle of NH_3 concentrations is very similar to the one of NO_2, with morning enhancements coincident with intensified road traffic. NH_3 evening enhancements synchronous with rush hours are also monitored in winter and fall. NH_3 concentrations measured during the weekends are consistently lower than NH_3 concentrations measured during weekdays in summer and fall. This is a further evidence of a significant traffic source of NH_3 in Paris.

1. Introduction

Ammonia (NH_3) is an air pollutant which plays a role ~~is involved~~ in important environmental and health issues [Rockström et al., 2009]. It is a highly reactive gas, with a lifetime of a few hours to a few days [Evangeliou et al., 2021; Dammers et al., 2019], capable of reacting with nitrogen oxides (NO_x) and sulfur oxides (SO_x) to form fine particulate matter composed of ammonium nitrate and ammonium sulfate [Sutton et al., 2013]. The formation of fine particles plays a major role in the degradation of air quality, as they are the cause of respiratory and cardiovascular diseases [Pope III et al., 2009].

Models have difficulty predicting events of particulate pollution associated with NH_3 since ground-based atmospheric observations of this gas are still relatively sparse [Nair and Yu, 2020] and difficult to implement [Twigg et al., 2022; von Bobrutzki et al., 2010]. To our knowledge, only six countries in the world (United States, China, the Netherlands, United Kingdom, Belgium, and Canada) have dedicated NH_3 observations in their atmospheric monitoring networks. This poses a problem for long-term monitoring of pollution and the implementation of emission reduction policies.

Global population growth causes increased food demand leading to higher ammonia emissions from intensive agricultural production systems [Fowler et al., 2013]. Global NH_3 emissions have increased by more than 80% between 1970 and 2017 [McDuffie et al., 2020]. In Europe, a substantial increase in nitrate and ammonium concentrations in the composition of fine articles has been observed for several years in the early spring when fertilizer applications intensify [Favez et al., 2021]. In addition, the share of emissions related to road traffic is also increasing because of popularization of catalytic converters in car engines [Zhang et al., 2021]. In France, 98% of ammonia comes from agricultural activities, via decomposition and volatilization of nitrogen fertilizers (34%) and animal waste (64%), the rest are from industry, road traffic and residential heating [CITEPA, 2022]. In the Ile-de-France region (Paris greater area), the share of agriculture is lower (75%) due to a higher contribution of traffic and residential sectors (13% and 12%, respectively [AirParif, 2022]). NH_3 emissions from road traffic are very poorly quantified and may be a larger than expected source in urban areas [Pu et al., 2023; Chatain et al., 2022; Cao et al., 2021; Roe et al., 2004; Sutton et al., 2000].

Monitoring NH_3 is therefore essential, especially in urban areas such as in Paris, where particulate pollution episodes are observed ~~monitored~~ almost every spring [Viatte et al., 2022] and often associated with emissions from agricultural activities in the surrounding areas [Viatte et al., 2021; Kutzner et al., 2021; Viatte et al., 2020; Petetin et al., 2016; Petit et al., 2015].

Global scale measurement of atmospheric ammonia is possible via soundings from several satellite-borne instruments such as AIRS [Warner et al., 2016], CrIS [Shephard and Cady-Pereira, 2015], and IASI [Clarisse et al., 2009]. Satellite measurements of atmospheric ammonia allow a description of its spatial distribution with global coverage. The detection of the multi-year evolution of concentrations is possible, as well as the detection of emission sources at the kilometer scale [Van Damme et al., 2018], and even the quantification of their variability~~ies~~ [Van Damme et al., 2021; Dammers et al., 2019]. Remote sensing data are also used as a mean to estimate ammonia emission inventories [Marais et al., 2021; Cao et al., 2020; Fortems-Cheiney et al., 2020].

Quantifying and analyzing temporal NH_3 variabilities at different scales (diurnal, weekly, seasonal, and interannual) helps to improve emission inventories and air quality forecasts [Cao et al., 2021]. Diurnal NH_3 variability, which is rarely measured, is particularly crucial because atmospheric models have difficulty representing it [Lonsdale et al., 2017]. NH_3 concentrations increase during the day due to the temperature dependence of emissions, but there may be many other factors at play influencing the diurnal variability of NH_3 concentrations in the atmosphere, such as transport, boundary layer height, deposition, fertilizer application time, road traffic emissions, and the interaction of all these factors [Sudesh and Kulshrestha, 2021; Osada, 2020; Wang et al., 2015]. The diurnal variability of NH_3, which is still largely missing from the ground and satellite observations, provides valuable information regarding sources, surface exchange, deposition, gas-particle conversion, and transport of NH_3 [Clarisse et al., 2021].

In this work, we present 2.5-years of atmospheric NH_3 concentrations measured in Paris using the synergy of ground-based and IASI satellite observations to quantify NH_3 variabilities at different time scales.

2. Methodology

2.1. mini-DOAS

NH_3 concentrations are measured since January 2020 in the Paris city-center (48.8°N, 2.3°E) using the ground-based miniDOAS instrument located at the QUALAIR super-site (40 meters above ground level, https://qualair.fr/index.php/en/english/). To the best of our knowledge this dataset constitutes the only continuous (day and night) NH_3 observations available at high temporal frequency representative of the Paris megacity. The miniDOAS (Diffential Optical Absorption Spectroscopy) is a state-of-art instrument suitable for NH_3 monitoring [Sintermann et al., 2016; Berkhout et al., 2017] since it performs accurate high temporal resolution measurements (every hour, day and night) [Volten et al., 2012]. It has been designed and developed by the National Institute for Public Health and the Environment (RIVM, Netherlands) to be part of the Dutch National Air Quality Monitoring Network [Berkhout et al., 2017]. The miniDOAS is an active remote sensing instrument based on open-path differential absorption spectrometry. It uses a xenon lamp which emits a UV light, ammonia having a strong absorption band in the UV between 200 and 230 nm. The UV light beam travels along an optical path of 20 m, at the end of which there is a reflector which reflects the UV light and sends it back to the spectrometer/receiver. The Beer-Lambert law is used to quantify the extinction at the absorption wavelengths of ammonia to retrieve atmospheric ammonia concentrations [Volten et al., 2012]. The miniDOAS can measure a wide range of ammonia concentrations (from 0.5 to 200 µg.m^{-3}) day and night and does not suffer from sampling artifacts, since it does not use a filter or inlet, unlike other commonly used instruments (such as Picarro, with no sampling artifacts, since it is not using any filter or inlet unlike other instruments [Caville et al., 2023; von Bobrutzki et al., 2010]). Estimated errors are 4.10^{-3} µg.m^{-3} on hourly measurements [Volten et al., 2012]. Using ammonia measurements performed from thise miniDOAS in Paris at the QUALAIR super-site (40 meters above ground level, https://qualair.fr/index.php/en/english/) in the Paris city-center, Viatte et al. (2021) demonstrated the contribution of NH_3 to particulate pollution events that occurredthe NH_3 contribution in particulate pollution events that occurred during the 2020 COVID lockdown has been demonstrated [Viatte et al., 2021].

2.2. IASI

The Infrared Atmospheric Sounding Interferometer (IASI, [Clerbaux et al., 2009]) was launched first in 2006 as part of the Metop satellite series to monitor atmospheric composition twice a day (at 9:30 and 21:30) globally. IASI measures atmospheric spectra in the thermal infrared region with an elliptical pixel footprint of 12 × 12 km at nadir and 20 × 39 km at the far end of the swath. In this study, we use

NH_3 columns derived from IASI morning (9:30) overpasses onboard Metop B and C from January 2020 to June 2022. When comparing IASI and miniDOAS NH_3 concentrations in Paris, we have selected coincident observations made within the same hour and the center of the IASI pixels was used to determine the distance between the miniDOAS and IASI measurements. In this work, we use version 3 of the ANNI-NH3 reanalyzed dataset [Van Damme et al., 2021; Guo et al., 2021; Viatte et al., 2022].

2.3. Meteorological data from ERA-5

Meteorological parameters originate from the ERA-5 database of the European Centre for Medium-Range Weather Forecasts (ECMWF, [Hersbach et al., 2020]), which is built from observations recalibrated into a global assimilation model at a 30 km resolution. ~~It is constituted from observations recalibrated on global data assimilation models at a 30km spatial resolution.~~ In this work, we used the hourly data of the temperature at 2 m, the precipitation, the u and v components of the wind at 100 m and the height of the boundary layer, taken from the grid cells in which Paris is located.

2.4. Back-trajectories and Potential Source Contribution Factor (PSCF) analysis

To study the transport affecting concentration of ammonia in Paris, we use the Hybrid Single-Particle Lagrangian Integrated Trajectory model (HYSPLIT, [Stein et al., 2015]) to calculate backward trajectories of air masses ending at altitudes of 100 m (above sea level which corresponds to the altitude of the miniDOAS location) between January 2020 and June 2022.

Meteorological data used in the runs are from the National Centers for Environmental Prediction (NCEP) / National Center for Atmospheric Research (NCAR) reanalysis at 2.5-degree global latitude-longitude projection. We ensure by visual inspections that the back trajectories using a 2.5° resolution meteorological dataset are similar to using a finer meteorological dataset at 0.25° resolution (GFS).

Due to the short and highly variable lifetime of NH_3, ranging between 2-4 hours [Dammers et al., 2019] and 12-hours [Evangeliou et al., 2021], we simulated an average 6-h backward trajectories with an interval of one hour. ~~Combining~~ Using the hourly NH_3 observations from the miniDOAS, the potential emission sources of NH_3 were analyzed. The Potential Source Contribution Factor (PSCF) method [Malm et al., 1986] is used to identify source regions affecting air quality in term of NH_3 concentration in Paris between January 2020 and June 2022. This method is now commonly used in atmospheric science [Wang et al., 2023; Qadri et al., 2022; Martino et al., 2022; Biuki et al., 2022; Ren et al., 2021; Zachary et al., 2018; Jeong et al., 2011] and combines the concentration dataset with air parcel back-trajectory to identify preferred pathways producing high observed NH_3 concentrations in Paris. The larger PSCF (range: 0–1), the greater contribution of the pollution region to the atmospheric pollutants at the receptor site.

3. Results

3.1. Comparison of NH_3 concentrations between IASI and mini-DOAS

The 2.5-years mean NH_3 total column distribution around Paris derived from IASI from January 1st 2020 to May 31st 2022 is shown in Figure 1 (top panel). To obtain averages at a high resolution needed for Greater Paris~~city~~-scale studies, we used the oversampling method described by van Damme et al. (2018) that takes into account the real elliptical sizes of each IASI pixel ~~[Van Damme et al., 2018]~~. All IASI maps shown in this study were computed using this methodology. Hot spots of ammonia are found around Paris in agricultural areas, especially in the Champagne-Ardennes region between Troyes and Reims cities [Viatte et al., 2020].

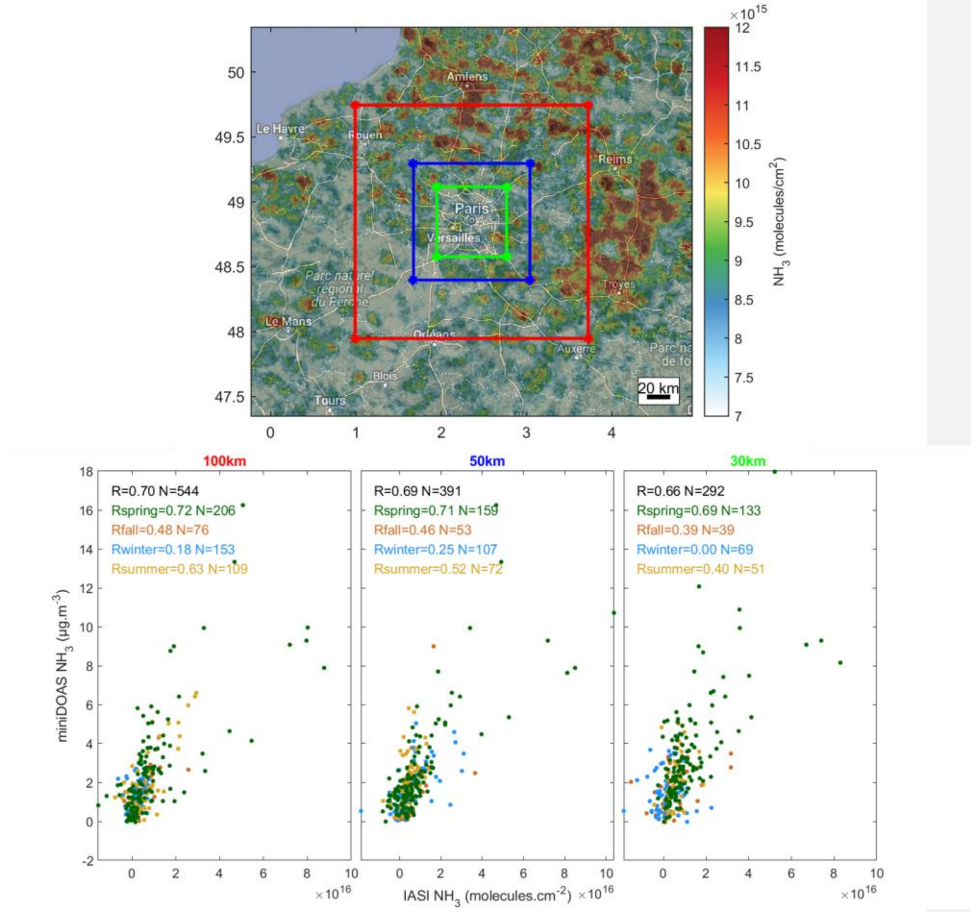

Figure 1: Top panel: 2.5-years average of IASI NH_3 column distributions (from January 1st 2020 to May 31st 2022). Bottom panel: miniDOAS ground-based NH_3 concentrations ($\mu g.m^{-3}$) versus IASI-retrieved NH_3 column concentrations ($molecules.cm^{-2}$) per season for different spatial criteria from Paris city center where the miniDOAS is located (100km in red box, 50km in blue box, and 30km green box).

NH_3 has a short atmospheric lifetime which is why we only compare miniDOAS data recorded within the same hour as the IASI morning overpass time. The IASI-retrieved column (in molecules.cm^{-2}) and the miniDOAS ground-based concentrations (µg.m^{-3}) are qualitatively compared to assess the spatial criteria (100km in red box, 50km in blue box, and 30km green box) and the season for which both datasets are in best agreement. In this study we are not converting IASI columns to surface observations since it introduces additional errors and does not change the correlation as explained in [Van Damme et al., 2015].

Overall, the miniDOAS and IASI NH_3 concentrations are in moderate agreement with Pearson correlation [Akoglu et al., 2018] of 0.70, 0.69, and 0.66 when considering IASI pixels within a 100km, 50km, and 30km box around Paris, respectively. The number of pairs is, however, reduced by a factor of two when considering IASI pixels in a 100km versus a 30km box around Paris. All correlations are significant (p-value < 0.05) except in winter for the 100km and 30km boxes, and in fall for the 30km box. The best agreement between the miniDOAS and IASI is in spring, with Pearson correlations ranging from 0.72 to 0.69 (green points in scatter plots of Figure 1). This period corresponds to high atmospheric NH_3 concentrations when spreading practices occur in the surrounding agricultural regions of Paris [Viatte et al., 2022]. The high correlation in spring between the two datasets can be attributed to two factors: 1) NH_3 concentrations are higher and therefore the signal measured by the two instruments are larger leading to a better correlation from the wide range of NH_3 concentrations (0-18 µg.m^{-3} for the miniDOAS and 0-1.10^{16} molecules.cm^{-2} for IASI, Figure 1) and 2) the high amount of NH_3 emitted in spring in the surrounding regions due to fertilizer applications can be transported to Paris [Viatte et al., 2022; Viatte et al., 2021] resulting in high correlations between the ~12-km IASI footprints and the local miniDOAS observations. In fall and summer, the Pearson correlation coefficients range from 0.63 to 0.40 between IASI and the miniDOAS for all boxes sizes. The lower correlations between the ground-based and the satellite NH_3 observations could reveal specific NH_3 sources in the close vicinity of the miniDOAS which might be not representative of the IASI pixels size. In winter, the agreements are poor between the miniDOAS and IASI because NH_3 concentrations are weak and IASI is less sensitive to lower atmospheric layers when thermal contrast is low [Van Damme et al., 2014]. In addition, we demonstrate that correlations between satellite and ground-based NH_3 observations are independent of atmospheric temperature and planetary boundary layer height (PBLH, Figure S1).

A trade-off between good correlations and keeping a sufficient number of collocations is found when comparing NH_3 concentrations from ground-based measurements located in the Paris city-center with the IASI dataset in a 50 km box. We chose for the rest of the analysis IASI dataset within the 50 km box to analyze spatiotemporal variabilities of NH_3 in Paris.

3.2. Impact of agriculture on NH_3 concentrations in Paris

3.2.1 2.5-years of NH_3 measurements in Paris

Here, we investigate temporal variabilities of NH_3 using 2.5-years of hourly measurements from January 1st 2020 to May 31st 2022 (Figure 2). The miniDOAS was working almost full time during this period with 16 888 hourly measurements, out of the 21 145 possible. The missing data is due either to some technical issues during warm conditions (malfunctioning aircondition in August 2021) or due to its removal from the QUALAIR facility for field measurement campaigns (from September 15th 2021 to November 24th 2021). Over the 16 888 hourly NH_3 measurements, average errors are 2.8 10^{-3} µg.m^{-3}

with maximum values occurring when signal is low due to a transient poor alignment (such as in April 2020, yellow dots in Figure 2). Description of the measurement uncertainties can be found in Volten et al. (2012).

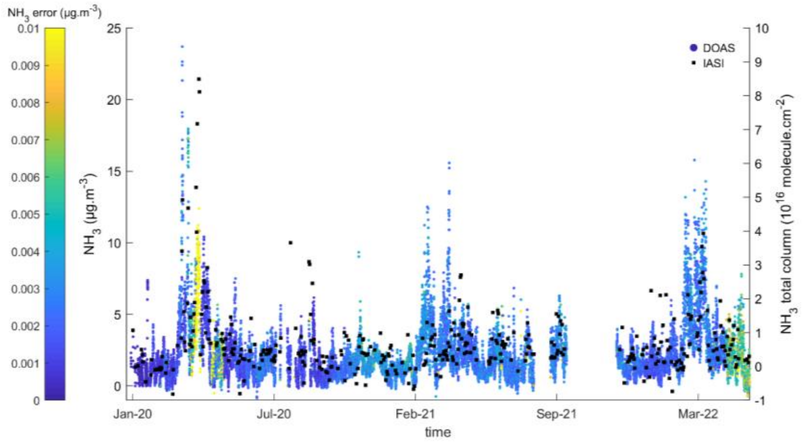

Figure 2: Timeseries of hourly NH_3 concentrations (in $\mu g.m^{-3}$) color coded by the errors on measurements derived from the miniDOAS located in Paris, and IASI NH_3 total columns (in black, $molecule.cm^{-2}$) observed in a 50km box centered in Paris from January 1st 2020 to May 31st 2022.

The measurements made by the miniDOAS over the period January 2020 - June 2022 (N=16 888) show an average ammonia concentration of 2.23 $\mu g.m^{-3}$ in Paris over this period, with a standard deviation of 2.02 $\mu g.m^{-3}$, indicating a high NH_3 variability. In comparison, the average concentration measured by the miniDOAS in an agricultural site at Grignon [Loubet et al., 2022] in September-October 2021 (France) is 6.52 ± 8.44 $\mu g.m^{-3}$ [Claville et al., 2023], almost three times higher than in Paris. The relatively low concentrations observed in Paris are explained by the distance to the major emission sources which are related to agricultural activities. Ammonia concentrations measured in Paris are on average lower or equivalent to those documented in urban areas such as Beijing (China, average of 21 ± standard deviation of 14 ppb corresponding to 14.7 ± 10 $\mu g.m^{-3}$ from January 2018 to January 2019, [Lan et al., 2021]), Shanghai (China, 6.2 ± 4.6 ppb which corresponds to 4.3 ± 3.2 $\mu g.m^{-3}$ from July 2013 to September 2014, [Wang et al., 2015]), Rome (Italy, 1.2–21.6 $\mu g.m^{-3}$ between May 2001 and March 2002, [Perrino et al., 2002]), Milan (Italy, 4.4–13.4 $\mu g.m^{-3}$ between 2007 and 2019, [Lonati et al., 2020]), Louisville (Unites-States, 2.2–5.2 $\mu g.m^{-3}$ from June to August 2011, [Li et al., 2017]) and Toronto (Canada, 2.5 ppb which corresponds to 1.75 $\mu g.m^{-3}$ from 2003 to 2011, [Hu et al. 2014]). The miniDOAS is located at an altitude of 40m so that its observation footprint is representative of the Greater Paris. This may partly explain the lower NH_3 concentrations observed in Paris compared to other urban areas.

The miniDOAS and IASI coincident measurements show relatively low interannual variability (Table 1). NH_3 annual concentrations measured by the miniDOAS are 2.06 ± 2.09 $\mu g.m^{-3}$ and 2.04 ± 1.56 $\mu g.m^{-3}$ for 2020 and 2021, respectively. The higher mean and standard deviation in 2022 (2.91 ± 2.40 $\mu g.m^{-3}$ for the miniDOAS) compared to the other years can be due the fact that measurements are performed from January to June only. IASI NH_3 total columns around Paris exhibit a higher NH_3 annual concentration and standard deviation in 2020 compared to the other years because of the multiple high pollution events ~~because of high pollution events~~ occurring in spring during the 2020-COVID lockdown as ~~-~~described in ~~(~~Viatte et al.~~,~~ (2021)~~)~~.

Table 1: Average NH_3 concentration, standard deviation, and number of observations for 2020, 2021 and part of 2022 derived from coincident measurements of the miniDOAS and IASI (50 km box around Paris).

years	2020		2021		2022	
	miniDOAS	IASI (50km)	miniDOAS	IASI (50km)	miniDOAS	IASI (50km)
NH_3 concentration (µg.m^{-3} or molecules.cm^{-2})	2.06	8.60 10^{15}	2.04	5.48 10^{15}	2.91	6.76 10^{15}
Standard deviation (µg.m^{-3} or molecules.cm^{-2})	2.09	1.58 10^{16}	1.56	5.69 10^{15}	2.40	9.35 10^{15}
Number of observations	7164	166	6182	134	3542	91

3.2.2 Seasonal and monthly NH_3 variabilities in Paris

Unlike the weak interannual variability of NH_3 concentrations in Paris, both ground-based (miniDOAS) and satellite (IASI) measurements reveal high seasonal variabilities of NH_3 concentrations (Figure 3). In spring, NH_3 concentration measured in Paris by the miniDOAS and IASI are on average 3.34 ± 2.67 µg.m^{-3} and 1.21x10^{16} ± 1.57x10^{16} molecules.cm^{-2}, respectively. These springtime NH_3 concentrations are enhanced by a factor of two compared to the other seasons, which is consistent with the fertilizer application periods over the nearby agricultural fields. Both datasets show that NH_3 concentrations in March and April are 2 to 3 times higher than the other months. Precipitation for these months is also lower than in February on average (see supplementary Figure S1~~2~~).

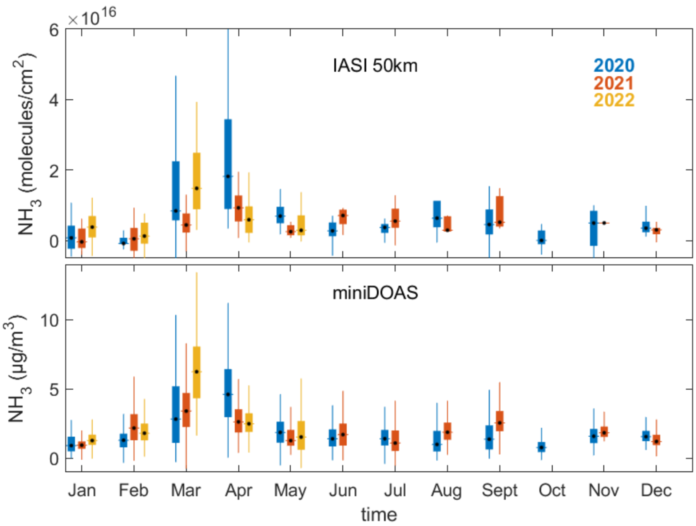

Figure 3: Monthly NH_3 concentrations color coded by the year of measurements (2020 in blue, 2021 in orange, and 2022 in yellow) derived from IASI (top panel, in molecules.cm^{-2}) in a 50km box around Paris

and the ground-based miniDOAS instrument (bottom panel, in µg.m^{-3}) located in Paris city-center. Note ~~One note~~ that IASI observations are only considered when a miniDOAS observation is available within the same hour than IASI overpass.

When considering each year of measurement separately, we notice that the timing of the maximum NH_3 concentrations is variable. In 2020, the maximum is reached in April with averaged NH_3 concentrations of 4.76 ± 2.48 µg.m^{-3} (miniDOAS) and 2.90x10^{16} ± 2.85x10^{16} molecules.cm^{-2} (IASI), whereas in 2022 the maximum appears in March with a monthly NH_3 concentration of 6.42 ± 2.46 µg.m^{-3} and 1.72x10^{16} ± 1.04x10^{16} molecules.cm^{-2} derived from the miniDOAS and IASI, respectively.

Meteorological conditions influence the timing of the agricultural practices (farmers do not spread their fertilizer when it rains), NH_3 volatilization from the soil to the atmosphere (higher temperature favors NH_3 volatilization [Sutton et al., 2013]), and the transport of NH_3 over Paris.

In April 2020, NH_3 concentrations observed by IASI and the miniDOAS are high compared to April 2022. In April 2020, precipitation is low (0.3 mm compared to 0.75mm in April 2022) and the monthly averaged atmospheric temperature is on 3 to 5°C higher than in 2021 and 2022 (Figure S1~~2~~). This could explain why NH_3 concentrations are higher in April 2020 than in 2022. Similarly, the lower ammonia concentration recorded in March 2021 compared to March 2022 is likely explained by higher precipitation (0.09 mm) and a lower temperature (of 2°C on monthly average) than in March 2022.

In 2021, a second NH_3 enhancement is measured in September by the miniDOAS (2.73 ± 1.14 µg.m^{-3}) and IASI (7.93x10^{15} ± 4.64x10^{15} molecules.cm^{-2}) which is not observed in 2020 possibly because atmospheric temperatures were lower than in 2021 (Figure S1). The pronounced seasonal variability can be explained in the first order by the practices of the farmers. In most European countries, strict regulations are applied in term of the timing of fertilizer application [Ge et al., 2020]. In France, it is forbidden to spread nitrogen fertilizers in winter months (between November 30th and February 15th, [Ludemann et al., 2022]) depending on fertilizer and land/crop types.

Overall, the seasonal and monthly variabilities of NH_3 concentrations in Paris are dominated by agricultural activities and meteorological conditions.

3.2.3 Potential Source Contribution Function (PSCF) analysis for NH_3 concentrations

To determine the origin of the NH_3 measured in Paris, the Potential Source Contribution Function (PSCF) is used. The PSCF analysis, as well as the IASI NH_3 maps, are shown for the investigated period (January 2020 – June 2022, Figure 4 upper panels), and in the spring of 2020, 2021~~for springs 2020, 2021~~, and 2022 (Figure 4, three lower panels).

Over the whole timeseries, the northeast (100 km from Paris in the Aisne department of France) and east (70km from Paris in the “Seine et Marne” department) locations are found to affect the NH_3 concentrations observed in the city between January 2020 and June 2022. These areas are indeed source regions of NH_3 according to coincident IASI observations (Figure 4, upper panels). According to wind fields parameters derived from ERA-5 over Paris (not shown here), the winds from the south are more intense (up to 18 m.s^{-1}) and are related to lower ammonia concentrations (between 0 and 4 µg.m^{-3}). The northern winds are on average weaker (maximum around 12 m.s^{-1}) and are associated with higher ammonia concentrations. In particular, for the northeast section the measured NH_3 concentration is found to exceed 8 µg.m^{-3}.

According to the PSCF analysis, the main sources of NH_3 from agricultural activities are found in the close areas of Paris (within 100 and 200 km from Paris city-center) mainly from the east and northeast directions. In France, the averaged utilized agricultural area per department in 2020 is 64.5 ha (Agreste – Recensements agricoles, https://stats.agriculture.gouv.fr/cartostat/#c=home). The highlighted departments by the PSCF analysis are ranked to have the most cultivated areas in France with 141.5 ha for Seine et Marne, 124.4 ha for Oise, and 110.4 ha for Aisne departments for instance.

Code de champ modifié

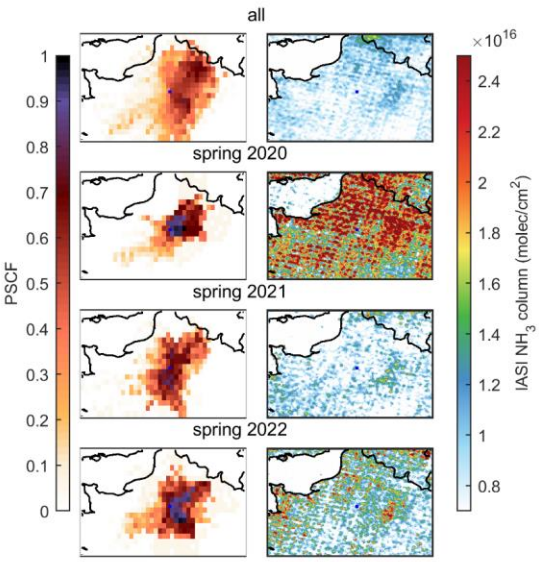

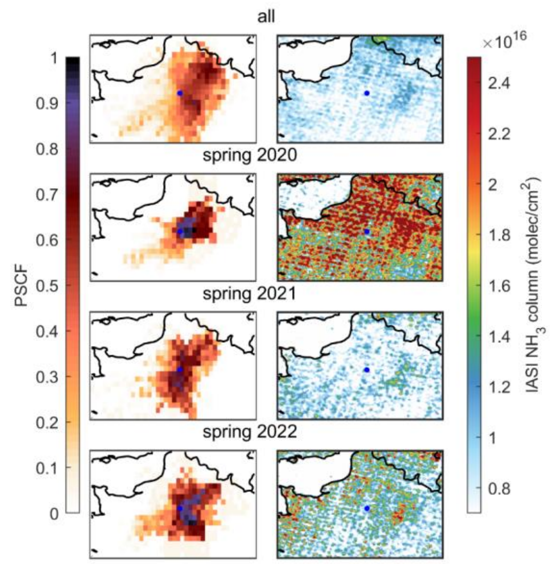

Figure 4: Potential Source Contribution Function (PSCF, left) and IASI NH_3 total columns (right, in molecules.cm^{-2}) The top row is the January 2020 to June 2022 average, and the 3 lower panels are for springs 2020, 2021, and 2022. The blue dot indicates the location of Paris.

In spring, when NH_3 concentrations are significantly higher in Paris (Figure 3) and in the surroundings (Figure 4 three lower right panels), the PSCF analysis show that the northeast and southeast regions are the major sources of the observed NH_3 concentrations in Paris. In spring 2020, NH_3 columns are higher than in spring 2021 and 2022, according to IASI observations. The main sources of NH_3 in spring 2020 are pronounced in the nearby east-northeast areas (at 50 km from Paris in the surrounding departments of Seine et Marne, Oise, and Val d'Oise). In spring 2021, IASI observations reveal lower NH_3 columns than in 2020 and 2022 and the sources of NH_3 concentrations in Paris are in the surrounding regions of Paris (100 km in all directions). In spring 2022, the northeast pathway is highlighted similarly to spring 2020 but with a contribution of the southeast region as well.

3.3 Effect of road traffic on NH_3 variability in Paris

3.3.1 Weekly cycle of NH_3 concentrations

The weekly cycles of ammonia concentrations measured in Paris by the miniDOAS and IASI over the studied timeseries are presented in Figure 5 (black bars, top panels). Both datasets show an increase of ammonia concentrations during the week, reaching a maximum on Thursday (2.21 µg.m^3 for the miniDOAS and 5.90x10^{15} molecules.cm^{-2} for IASI).

The weekly cycle of IASI measurements in Paris is almost analogous to the one observed over European agricultural areas with low concentrations observed on Mondays, as a result of reduced NH_3 emissions over the weekend, and an accumulation of ammonia during the week [Van Damme et al., 2022]. In addition, the IASI NH_3 weekly cycle averaged over 2.5-years of measurements in Paris is very similar to the NH_3 weekly cycle measured in spring (Figure 5) when agricultural activities intensify. Monitoring similar NH_3 weekly variability in the urban area of Paris demonstrates that agricultural activities in the surrounding areas control the variability of ammonia in Paris on average over the whole season.

The NH_3 weekly cycle observed over 2.5-years of measurements from the ground-based miniDOAS and the IASI satellite observations show, however, relatively low NH_3 concentrations on Saturday and Sunday. The cycle is less pronounced for IASI measurements. Ammonia concentrations observed over the weekend by the miniDOAS and IASI are lower by 25% and 20% compared to NH_3 concentrations averaged over the weekdays in Paris.

When considering intraweek variabilities by seasons (Figure 5, four lower panels), one can observe that both IASI and the miniDOAS dataset reveal similar NH_3 weekly cycles. The NH_3 miniDOAS measurements and coincident IASI total columns measured in a 50km box around Paris exhibit lower concentrations over the weekends compared to weekdays for all seasons, except in spring for which higher NH_3 concentrations are found on Wednesday and Sunday. In spring, the miniDOAS and IASI measure a difference of NH_3 concentrations averaged over the weekends compared to weekdays of +1% and -7%, respectively. In fall, summer, and winter, the miniDOAS (IASI) instrument measure a decrease of NH_3 concentrations between weekends and weekdays of 70% (34%), 42% (28%), and 27% (53%) respectively.

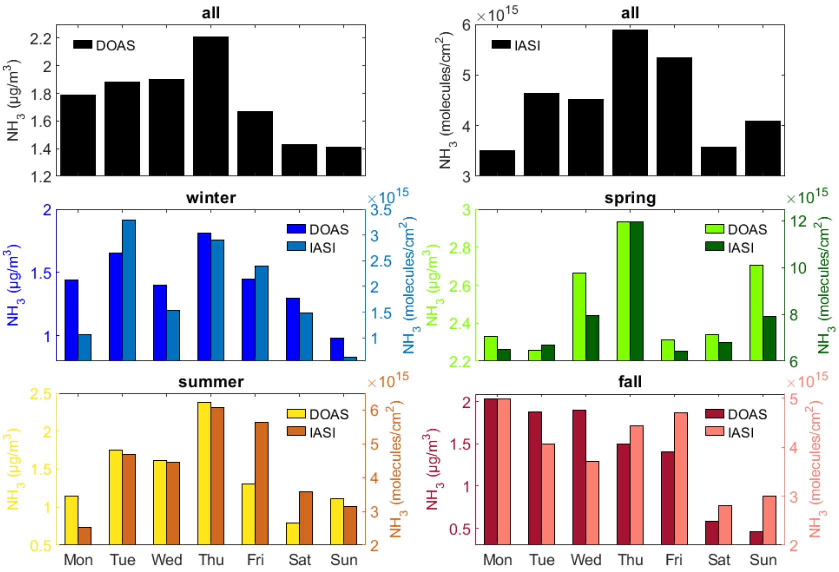

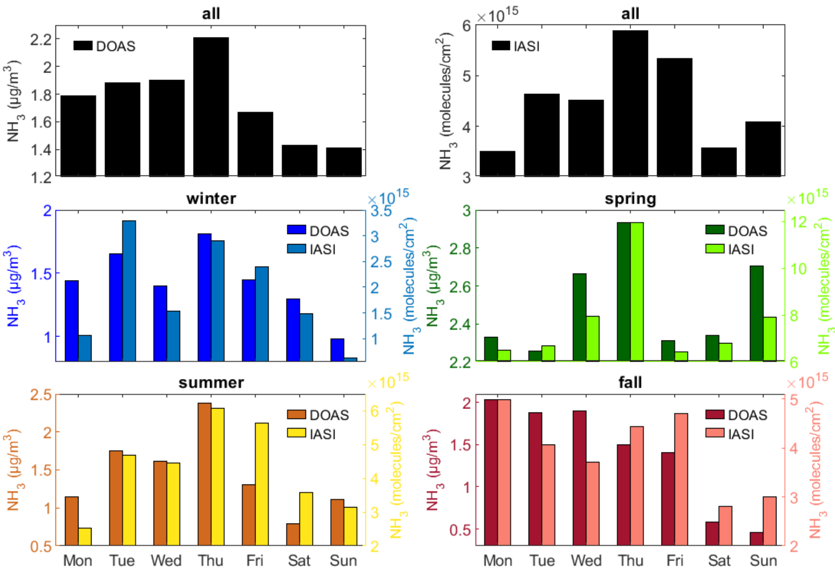

Figure 5: Day of the week NH_3 concentrations derived from the miniDOAS ($\mu g.m^{-3}$) and IASI ($molecules.cm^{-2}$) in Paris for the investigated period (January 2020 to May 2022, top panels), and for

different seasons (winter in blue, spring in green, summer in brown and yellow, and fall in red and pink bars).

Comparing these weekly variabilities with those of the weekly flow of cars in Paris (Figure S23), the same pattern is clearly highlighted with a stable number of cars per hour from Monday to Friday (around 640) and a decrease of 14% over the weekends.

We can make the hypothesis that during all seasons except spring, the influence of the agricultural practices on the variability of ammonia in Paris is less pronounced, revealing NH_3 contribution from the traffic source. Since the road traffic intensity is constant throughout the year in Paris, the proportion of ammonia emitted from road traffic is proportionally higher outside the fertilization period.

3.3.2 Diurnal cycle of NH_3 concentration in Paris

With the high temporal resolution of the mini-DOAS acquisitions, the diurnal variability of NH_3 concentration is assessed in Paris using, for the first time, a quasi-continuous (temporal coverage of 80%) and a relatively long timeseries of 2.5-years of NH_3 observations.

Hourly NH_3 concentrations measured by the miniDOAS from January 2020 to May 2022 are shown in Figure S34. It shows a marked diurnal variability of NH_3, with a decrease of about 30% in the middle of the day (around 14:00 LT) compared to the night, then an increase in the afternoon to reach again a maximum during the night.

Note that this diurnal variability of NH_3 measured by the miniDOAS is different than the one reported during springtime pollution episodes from a ground-based Fourrier Transform InfraRed spectrometer located in the suburbs of Paris [Kutzner et al., 2021]. While measured integrated NH_3 total columns show an intraday increase until late afternoon, the miniDOAS measures NH_3 concentrations varying in opposition to the boundary layer height (Figure S34). This reflects the dynamical effect of the boundary layer height, which is controlled by atmospheric temperature, on the dilution of pollutants concentrations measured close to the surface. Such effect is also seen with surface measurements of NO_2 concentrations in Paris (Figure S34).

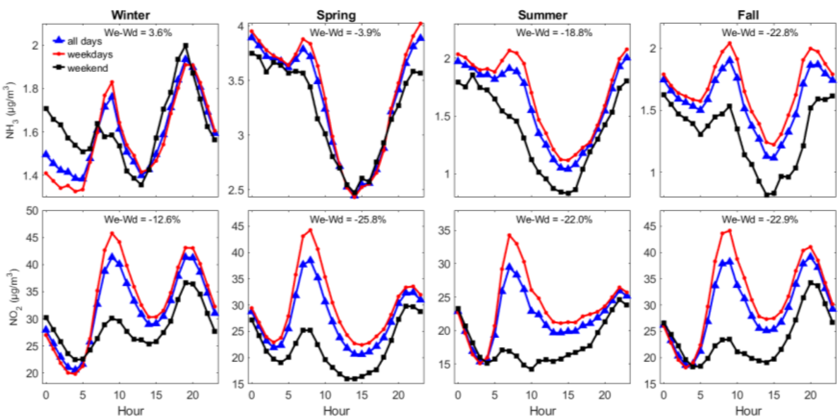

Figure 6: Diurnal variability of NH_3 (upper panels) and NO_2 (lower panels) concentrations measured by the miniDOAS and Airparif in (µg.m^{-3}) averaged by seasons using 2.5-years of measurements in Paris. Hours are indicated in local time. The diurnal variability of NH_3 and NO_2 are shown in blue lines when considering all days, in red lines for weekdays, and in black lines for weekends.

The diurnal variability of NH_3 concentrations presents an increase in the morning visible for all seasons (Figure 6). Between 5:00 and 8:00, road-traffic in Paris increases by a factor 4 (Figure S2~~3~~) and NH_3 concentrations rise by more than 20% in winter and fall, and about 3% in summer and spring.

To verify the hypothesis that road traffic is responsible for these morning enhancements, NO_2 diurnal variability is also shown in Figure 6 (lower panels). In Paris, NO_2 is considered as a proxy for road traffic emissions [Pazmino et al., 2022]. For all seasons, morning enhancements of NO_2 concentrations related to intensified road traffic emissions are coincident with morning enhancements of NH_3 concentrations. Similarly, enhancements of NO_2 and NH_3 concentrations are observed during the evenings (20:00 to 22:00 LT) in winter and fall only. In spring, agriculture which is the overall dominant source of ammonia in Paris, prevents from monitoring NH_3 emitted from road traffic. Conversely, in fall and winter, the relative share of agriculture is weaker, and the peaks of NH_3 concentrations during rush hours (morning and evening) are clearly observed by the miniDOAS.

Diurnal variability of NH_3 and NO_2 concentrations averaged during weekdays (red lines) and weekends (black lines) are shown in Figure 6. NO_2 concentrations are systematically lower during weekends by 12.6%, 25.8%, 22.0%, and 22.9% in winter, spring, summer, and fall respectively, compared to weekdays. Similarly, diurnal cycle of NH_3 concentrations averaged during weekends are constantly lower than NH_3 concentrations averaged during weekdays in summer and fall by 22.0% and 22.9%.

This highlights the importance of traffic emissions of NH_3 in such urban area of Paris, detected by ground-based measurements when agricultural practices are reduced in the surrounding region.

These results are consistent with previous studies showing the importance of NH_3 emissions from traffic in urban areas, such as in Rome (Italy, [Perrino et al., 2002]), in Beijing (China, [Ianniello et al., 2010]), in Shanghai (China, [Wang et al., 2015]), and in Manchester (United Kingdom, [Whitehead et al., 2004]) for instance. These emissions have gradually become another major contribution of ammonia pollution in urban areas in the United States and China [Sun et al., 2017]. Ammonia emissions from road vehicles are shown to be underestimated in the United Kingdom [Farren et al., 2020] and in densely-populated areas in China [Wen at al., 2022]. In France, NH_3 levels measured at a traffic site of Reims city are significantly higher than those observed in a background site [Chatain et al., 2022]. Our results in Paris confirm that traffic has a significant contribution to atmospheric nitrogen budgets and stress the need for further NH_3 monitoring in urban sites.

4. Conclusion

~~Atmospheric~~ Temporal variabilities of NH_3 concentrations in Paris are assessed using joint~~ted~~ observations of ground-based (miniDOAS) and satellite (IASI) remote sensing observations from January 2020 to June 2022. We present the first relatively long (2.5-years) and continuous record of hourly NH_3 concentrations in Paris to determine temporal variabilities of ammonia at different scales (from interannual to diurnal variability) to unravel emission sources (traffic and agriculture).

Qualitative comparison of NH_3 derived from the ground-based miniDOAS located in Paris city-center and IASI satellite observations reveals an overall moderate agreement with Pearson's correlation coefficients of 0.66, 0.69 and 0.70 when considering IASI observations in a 100km, 50km, and 30km box around Paris. The best agreement between both datasets is found during springtime when NH_3 concentrations are 2 to 3 times higher than during the other seasons due to fertilizer spreading due to spreading practices occurring in the surrounding agricultural regions of Paris. Overall, agricultural activities driven by favorable meteorological conditions (high temperature and low precipitation) control the seasonal and monthly variabilities of NH_3 in Paris. The PSCF analyses indicate that the agricultural regions to the east and northeast within 100 to 200 km from Paris city-center have the greatest impact on the NH_3 budget in ParisThe PSCF analyses indicate that the close east and northeast agricultural regions (within 100 and 200 km from Paris city-center) affect the most the NH_3 budget in Paris.

Road-traffic emissions are noticeable in the weekly NH_3 cycles measured by satellite and ground-based instruments, when agricultural related emissions are weak. Ammonia concentrations observed over the weekend by the miniDOAS and IASI are lower by 25% and 20% compared to NH_3 concentrations averaged over the weekdays. In addition, diurnal cycles of NH_3 concentrations in Paris are similar to NO_2 and reveal coincident enhancements during rush hours. Further long-term NH_3 monitoring in urban areas is needed to better estimate NH_3 emissions from the on-road sector and their impact on secondary particle formation.

We have shown that the planetary boundary layer height greatly influences diurnal variabilities derived from surface measurements. Future work will be carried to compare these NH_3 datasets in Paris to atmospheric model outputs to evaluate the timing and the absolute value of emission inventories, as well as the partition between NH_3 emission sectors (traffic vs. agriculture). The launch of the geostationary MTG satellite carrying the hyperspectral sounder IRS, scheduled for 2024, will offer unprecedent atmospheric observations with a spatial resolution of 4 km × 4 km (at the Equator) and a high temporal resolution (every 30 minutes over Europe). These new observations will improve our understanding of the diurnal variability of ammonia, and it will be a great addition to the miniDOAS and IASI observations.

Data availability

The IASI NH_3 dataset used in this study are available via the Zenodo repository https://doi.org/10.5281/zenodo.7962362 (Viatte, 2023). The miniDOAS data are available here https://iasi-ft.eu/products/nh3_minidoas/ (Viatte, 2023). The ERA-5 data are available via the Climate Data Record (CDR) Copernicus website https://cds.climate.copernicus.eu/cdsapp#!/search?text=ERA5%20back%20extension&type=dataset (C3S CDS, 2023). The potential source contribution function is available via the Meteothink.org http://meteothink.org/docs/trajstat/pscf.html (Wang et al., 2009). Last access to all URLs: 23 May 2023.

Code de champ modifié

Code de champ modifié

Code de champ modifié

Code de champ modifié

Author contributions

CV and NG designed the project. MVD and LC provided the IASI data. AH, AW, DS helped with the miniDOAS installation and data acquisition. CV and CD analyzed the data. CV and CD wrote the manuscript draft. All the co-authors reviewed and edited the manuscript. CC wrote proposals to financially support the miniDOAS.

Competing interests

The authors declare that they have no conflict of interest.

Acknowledgments

IASI is a joint mission of EUMETSAT and the Centre National d'Etudes Spatiales (CNES, France). The IASI Level 1C data are distributed in near real time by EUMETSAT through the EUMETCast system distribution. The authors acknowledge the AERIS data infrastructure (https://www.aeris-data.fr) for providing access to the IASI Level 1 radiance and Level 2 NH_3 concentration data used in this study. CNES and the AC-SAF (CDOP3) project provided financial support for the miniDOAS acquisition. We thank the NOAA's Air Resources Laboratory (ARL) for providing the HYSPLIT model. Research at ULB was supported by the Belgian State Federal Office for Scientific, Technical and Cultural Affairs (Prodex HIRS) and the Air Liquide Foundation (TAPIR project). LC is Research Associate supported by the Belgian F.R.S.-FNRS. MVD is supported by the FED-tWIN project ARENBERG funded via the Belgian Science Policy Office (BELSPO).

References

AERIS: NH3 total column from IASI (Level 2), https://iasi.aeris-data.fr/NH3/, last access: 11 May 2023.

Airparif, 2022 : https://www.airparif.asso.fr/surveiller-la-pollution/les-emissions, last access 24 Feb 2023.

Code de champ modifié

Akoglu, H.: User's guide to correlation coefficients, Turkish J. Emerg. Med., 18(3), 91–93, doi:https://doi.org/10.1016/j.tjem.2018.08.001, 2018.

Berkhout, A. J. C., Swart, D. P. J., Volten, H., Gast, L. F. L., Haaima, M., Verboom, H., Stefess, G., Hafkenscheid, T., and Hoogerbrugge, R.: Replacing the AMOR with the miniDOAS in the ammonia monitoring network in the Netherlands, Atmos. Meas. Tech., 10, 4099–4120, https://doi.org/10.5194/amt-10-4099-2017, 2017.

Biuki, Z. A., Parvin, P. and Aghaei, M.: Satellite remote sensing of particulate matter in the atmosphere of megacities: A case study of Tehran, Iran, Atmos. Pollut. Res., 13(10), 101545, doi:https://doi.org/10.1016/j.apr.2022.101545, 2022.

Cao, H., Henze, D. K., Cady-Pereira, K., McDonald, B. C., Harkins, C., Sun, K., Bowman, K. W., Fu, T.-M. and Nawaz, M. O.: COVID-19 Lockdowns Afford the First Satellite-Based Confirmation That Vehicles Are an Under-recognized Source of Urban NH3 Pollution in Los Angeles, Environ. Sci. Technol. Lett., doi:10.1021/acs.estlett.1c00730, 2021.

Cao, H., Henze, D. K., Shephard, M. W., Dammers, E., Cady-Pereira, K., Alvarado, M., Lonsdale, C., Luo, G., Yu, F., Zhu, L., Danielson, C. G. and Edgerton, E. S.: Inverse modeling of NH3 sources using CrIS remote sensing measurements, Environ. Res. Lett., 15(10), 104082, doi:10.1088/1748-9326/abb5cc, 2020.

Caville et al.: Measurements of ammonia in ambient air and over a controlled artificial source during the AMICA field campaign at a rural site in the Ile-de-France region, Sensors, to be submitted, 2023.

Chatain, M., Chretien, E., Crunaire, S. and Jantzem, E.: Road Traffic and Its Influence on Urban Ammonia Concentrations (France), Atmosphere (Basel)., 13(7), doi:10.3390/atmos13071032, 2022.

CITEPA, 2022: https://www.citepa.org/wp-content/uploads/publications/cee-nu/UNECE_France_mars2022.pdf, last access 24 Feb 2023.

Code de champ modifié

Clarisse, L., Van Damme, M., Hurtmans, D., Franco, B., Clerbaux, C., & Coheur, P.-F.: The diel cycle of NH3 observed from the FY-4A Geostationary Interferometric Infrared Sounder (GIIRS). Geophysical Research Letters, 48, e2021GL093010, https://doi.org/10.1029/2021GL093010, 2021.

Clarisse, L., Clerbaux, C., Dentener, F., Hurtmans, D., and Coheur, P.-F.: Global ammonia distribution derived from infrared satellite observations, Nat. Geosci., 2, 479–483, https://doi.org/10.1038/ngeo551, 2009.

Clerbaux, C., Boynard, A., Clarisse, L., George, M., Hadji-Lazaro, J., Herbin, H., Hurtmans, D., Pommier, M., Razavi, A., Turquety, S., Wespes, C. and Coheur, P.-F.: Monitoring of atmospheric composition using the thermal infrared IASI/MetOp sounder, Atmos. Chem. Phys., 9(16), 6041–6054, doi:10.5194/acp-9-6041-2009, 2009.

Copernicus Climate Change Service, Climate Data Store, (2023): ERA5 hourly data on single levels from 1940 to present. Copernicus Climate Change Service (C3S) Climate Data Store (CDS), DOI: 10.24381/cds.adbb2d47 (Accessed on 11-May-2023)

Dammers, E., McLinden, C. A., Griffin, D., Shephard, M. W., Van Der Graaf, S., Lutsch, E., Schaap, M., Gainairu-Matz, Y., Fioletov, V., Van Damme, M., Whitburn, S., Clarisse, L., Cady-Pereira, K., Clerbaux, C., Coheur, P. F., and Erisman, J. W.: NH3 emissions from large point sources derived from CrIS and IASI satellite observations, Atmos. Chem. Phys., 19, 12261–12293, https://doi.org/10.5194/acp-19-12261-2019, 2019.

Evangeliou, N., Balkanski, Y., Eckhardt, S., Cozic, A., Van Damme, M., Coheur, P.-F., Clarisse, L., Shephard, M. W., Cady-Pereira, K. E. and Hauglustaine, D.: 10-year satellite-constrained fluxes of ammonia improve performance of chemistry transport models, Atmos. Chem. Phys., 21(6), 4431–4451, doi:10.5194/acp-21-4431-2021, 2021.

Farren, N. J., Davison, J., Rose, R. A., Wagner, R. L. and Carslaw, D. C.: Underestimated Ammonia Emissions from Road Vehicles, Environ. Sci. Technol., 54(24), 15689–15697, doi:10.1021/acs.est.0c05839, 2020.

Favez, O., Weber, S., Petit, J.-E., Alleman, L. Y., Albinet, A., Riffault, V., Chazeau, B., Amodeo, T., Salameh, D., Zhang, Y., Srivastava, D., Samaké, A., Aujay-Plouzeau, R., Papin, A., Bonnaire, N., Boullanger, C., Chatain, M., Chevrier, F., Detournay, A., Leoz-Garziandia, E. (2021). Overview of the French Operational Network for In Situ Observation of PM Chemical Composition and Sources in Urban Environments (CARA Program), Atmosphere, 12(2), https://doi.org/10.3390/atmos12020207, 2021.

Fortems-Cheiney, A., Dufour, G., Dufossé, K., Couvidat, F., Gilliot, J.-M., Siour, G., Beekmann, M., Foret, G., Meleux, F., Clarisse, L., Coheur, P.-F., Van Damme, M., Clerbaux, C., and Génermont, S.: Do alternative inventories converge on the spatiotemporal representation of spring ammonia emissions in France?, Atmos. Chem. Phys., 20, 13481–13495, https://doi.org/10.5194/acp-20-13481-2020, 2020.

Fowler, D., et al.: The global nitrogen cycle in the twenty-first century, Philos. Trans. R. Soc. B, 368(1621), 1–13, doi:10.1098/rstb.2013.0164, 2013.

Ge, X., Schaap, M., Kranenburg, R., Segers, A., Reinds, G. J., Kros, H. and de Vries, W.: Modeling atmospheric ammonia using agricultural emissions with improved spatial variability and temporal dynamics, Atmos. Chem. Phys., 20(24), 16055–16087, doi:10.5194/acp-20-16055-2020, 2020.

Guo, X., Wang, R., Pan, D., Zondlo, M. A., Clarisse, L., Van Damme, M., Whitburn, S., Coheur, P.-F., Clerbaux, C., Franco, B., Golston, L. M., Wendt, L., Sun, K., Tao, L., Miller, D., Mikoviny, T., Müller, M., Wisthaler, A., Tevlin, A. G., Murphy, J. G., Nowak, J. B., Roscioli, J. R., Volkamer, R., Kille, N., Neuman, J. A., Eilerman, S. J., Crawford, J. H., Yacovitch, T. I., Barrick, J. D. and Scarino, A. J.: Validation of IASI Satellite Ammonia Observations at the Pixel Scale Using In Situ Vertical Profiles, J. Geophys. Res. Atmos., 126(9), e2020JD033475, doi:https://doi.org/10.1029/2020JD033475, 2021.

Hersbach, H.; Bell, B.; Berrisford, P.; Hirahara, S.; Horányi, A.; Muñoz-Sabater, J.; Nicolas, J.; Peubey, C.; Radu, R.; Schepers, D.; et al. The ERA5 global reanalysis. *Q. J. R. Meteorol. Soc. 146*, 1999–2049, doi:10.1002/qj.3803, https://www.ecmwf.int/en/forecasts/datasets/reanalysis-datasets/era5, 2020.

Hu, Q., Zhang, L., Evans, G. J. and Yao, X.: Variability of atmospheric ammonia related to potential emission sources in downtown Toronto, Canada, Atmos. Environ., 99, 365–373, doi:https://doi.org/10.1016/j.atmosenv.2014.10.006, 2014.

Ianniello, A., Spataro, F., Esposito, G., Allegrini, I., Rantica, E., Ancora, M. P., Hu, M. and Zhu, T.: Occurrence of gas phase ammonia in the area of Beijing (China), Atmos. Chem. Phys., 10(19), 9487–9503, doi:10.5194/acp-10-9487-2010, 2010.

Jeong, U., Kim, J., Lee, H., Jung, J., Kim, Y. J., Song, C. H. and Koo, J.-H.: Estimation of the contributions of long range transported aerosol in East Asia to carbonaceous aerosol and PM concentrations in Seoul{,} Korea using highly time resolved measurements: a PSCF model approach, J. Environ. Monit., 13(7), 1905–1918, doi:10.1039/C0EM00659A, 2011.

Kutzner, R. D., Cuesta, J., Chelin, P., Petit, J.-E., Ray, M., Landsheere, X., Tournadre, B., Dupont, J.-C., Rosso, A., Hase, F., Orphal, J., and Beekmann, M.: Diurnal evolution of total column and surface atmospheric ammonia in the megacity of Paris, France, during an intense springtime pollution episode, Atmos. Chem. Phys., 21, 12091–12111, https://doi.org/10.5194/acp-21-12091-2021, 2021.

Lan, Z., Lin, W., Pu, W. and Ma, Z.: Measurement report: Exploring NH_3 behavior in urban and suburban Beijing: comparison and implications, Atmos. Chem. Phys., 21(6), 4561–4573, doi:10.5194/acp-21-4561-2021, 2021.

Li, Y., Thompson, T. M., Van Damme, M., Chen, X., Benedict, K. B., Shao, Y., Day, D., Boris, A., Sullivan, A. P., Ham, J., Whitburn, S., Clarisse, L., Coheur, P.-F. and Collett Jr., J. L.: Temporal and spatial variability of ammonia in urban and agricultural regions of northern Colorado, United States, Atmos. Chem. Phys., 17(10), 6197–6213, doi:10.5194/acp-17-6197-2017, 2017.

Lonati, G. and Cernuschi, S.: Temporal and spatial variability of atmospheric ammonia in the Lombardy region (Northern Italy), Atmos. Pollut. Res., 11(12), 2154–2163, doi:https://doi.org/10.1016/j.apr.2020.06.004, 2020.

Lonsdale, C. R., Hegarty, J. D., Cady-Pereira, K. E., Alvarado, M. J., Henze, D. K., Turner, M. D., Capps, S. L., Nowak, J. B., Neuman, J. A., Middlebrook, A. M., Bahreini, R., Murphy, J. G., Markovic, M. Z., VandenBoer, T. C., Russell, L. M., and Scarino, A. J.: Modeling the diurnal variability of agricultural ammonia in Bakersfield, California, during the CalNex campaign, Atmos. Chem. Phys., 17, 2721–2739, https://doi.org/10.5194/acp-17-2721-2017, 2017.

Loubet, B., Buysse, P., Gonzaga-Gomez, L., Lafouge, F., Ciuraru, R., Decuq, C., Kammer, J., Bsaibes, S., Boissard, C., Durand, B., Gueudet, J.-C., Fanucci, O., Zurfluh, O., Abis, L., Zannoni, N., Truong, F., Baisnée, D., Sarda-Estève, R., Staudt, M. and Gros, V.: Volatile organic compound fluxes over a winter wheat field by PTR-Qi-TOF-MS and eddy covariance, Atmos. Chem. Phys., 22(4), 2817–2842, doi:10.5194/acp-22-2817-2022, 2022.

Ludemann, C. I., Gruere, A., Heffer, P. and Dobermann, A.: Global data on fertilizer use by crop and by country, Sci. Data, 9(1), 501, doi:10.1038/s41597-022-01592-z, 2022.

Malm, W. C., Johnson, C. E., and Bresch, J. F.: Application of principal component analysis for purpose of identifying source receptor relationships, in Receptor Methods for Source Apportionment, Pace, T.G., Ed.; Publication TR-5, Air Pollution Control Association, Pittsburgh, PA, pp. 127–148, 1986.

Marais, E. A., Pandey, A. K., Van Damme, M., Clarisse, L., Coheur, P.-F., Shephard, M. W., Cady-Pereira, K. E., Misselbrook, T., Zhu, L., Luo, G. and Yu, F.: UK Ammonia Emissions Estimated With Satellite

Observations and GEOS-Chem, J. Geophys. Res. Atmos., 126(18), e2021JD035237, doi:https://doi.org/10.1029/2021JD035237, 2021.

Martino, M., Tassone, A., Angiuli, L., Naccarato, A., Dambruoso, P. R., Mazzone, F., Trizio, L., Leonardi, C., Petracchini, F., Sprovieri, F., Pirrone, N., D'Amore, F. and Bencardino, M.: First atmospheric mercury measurements at a coastal site in the Apulia region: seasonal variability and source analysis, Environ. Sci. Pollut. Res., 29(45), 68460–68475, doi:10.1007/s11356-022-20505-6, 2022.

McDuffie, E. E., Smith, S. J., O'Rourke, P., Tibrewal, K., Venkataraman, C., Marais, E. A., Zheng, B., Crippa, M., Brauer, M., and Martin, R. V.: A global anthropogenic emission inventory of atmospheric pollutants from sector- and fuel-specific sources (1970–2017): an application of the Community Emissions Data System (CEDS), Earth Syst. Sci. Data, 12, 3413–3442, https://doi.org/10.5194/essd-12-3413-2020, 2020.

Nair, A. A. and Yu, F.: Quantification of Atmospheric Ammonia Concentrations: A Review of Its Measurement and Modeling, Atmosphere (Basel)., 11(10), doi:10.3390/atmos11101092, 2020.

Osada, K.: Measurement report: Short-term variation in ammonia concentrations in an urban area increased by mist evaporation and emissions from a forest canopy with bird droppings, Atmos. Chem. Phys., 20, 11941–11954, https://doi.org/10.5194/acp-20-11941-2020, 2020.

Pazmiño, A., Beekmann, M., Goutail, F., Ionov, D., Bazureau, A., Nunes-Pinharanda, M., Hauchecorne, A., and Godin-Beekmann, S.: Impact of the COVID-19 pandemic related to lockdown measures on tropospheric NO_2 columns over Île-de-France, Atmos. Chem. Phys., 21, 18303–18317, https://doi.org/10.5194/acp-21-18303-2021, 2021.

Perrino, C., Catrambone, M., Di Menno Di Bucchianico, A. and Allegrini, I.: Gaseous ammonia in the urban area of Rome, Italy and its relationship with traffic emissions, Atmos. Environ., 36(34), 5385–5394, doi:https://doi.org/10.1016/S1352-2310(02)00469-7, 2002.

Petetin, H., et al.: Assessing the ammonium nitrate formation regime in the Paris megacity and its representation in the CHIMERE model, Atmos. Chem. Phys., 16, 10419-10440, doi:10.5194/acp-16-10419-2016, 2016.

Petit, J.-E., Favez, O., Sciare, J., Crenn, V., Sarda-Estève, R., Bonnaire, N., Močnik, G., Dupont, J.-C., Haeffelin, M., and Leoz-Garziandia, E.: Two years of near real-time chemical composition of submicron aerosols in the region of Paris using an Aerosol Chemical Speciation Monitor (ACSM) and a multi-wavelength Aethalometer, Atmos. Chem. Phys., 15, 2985–3005, https://doi.org/10.5194/acp-15-2985-2015, 2015.

Pu, W., Sheng, J., Tian, P., Huang, M., Liu, X., Collett, J. L., Li, Z., Zhao, X., He, D., Dong, F., Zhang, N., Quan, W., Qiu, Y., Song, Y., Lin, W., Pan, Y. and Ma, Z.: On-road mobile mapping of spatial variations and source contributions of ammonia in Beijing, China, Sci. Total Environ., 864, 160869, doi:https://doi.org/10.1016/j.scitotenv.2022.160869, 2023.

Pope III, C. A., et al.: Fine-particulate air pollution and life expectancy in the United States, N. Engl. J. Med., 360(4), 376–386, doi:10.1056/NEJMsa0805646, 2009.

Qadri, A. M., Singh, G. K., Paul, D., Gupta, T., Rabha, S., Islam, N. and Saikia, B. K.: Variabilities of δ13C and carbonaceous components in ambient PM2.5 in Northeast India: Insights into sources and atmospheric processes, Environ. Res., 214, 113801, doi:https://doi.org/10.1016/j.envres.2022.113801, 2022.

Ren, B., Xie, P., Xu, J., Li, A., Tian, X., Hu, Z., Huang, Y., Li, X., Zhang, Q., Ren, H. and Ji, H.: Use of the PSCF method to analyze the variations of potential sources and transports of NO2, SO2, and HCHO observed by MAX-DOAS in Nanjing, China during 2019, Sci. Total Environ., 782, 146865, doi:https://doi.org/10.1016/j.scitotenv.2021.146865, 2021.

Rockström, J., Steffen, W., Noone, K., Persson, Å., Chapin, F. S., Lambin, E. F., Lenton, T. M., Scheffer, M., Folke, C., Schellnhuber, H. J., Nykvist, B., de Wit, C. A., Hughes, T., van der Leeuw, S., Rodhe, H., Sörlin, S., Snyder, P. K., Costanza, R., Svedin, U., Falkenmark, M., Karlberg, L., Corell, R. W., Fabry, V. J., Hansen, J., Walker, B., Liverman, D., Richardson, K., Crutzen, P. and Foley, J. A.: A safe operating space for humanity, Nature, 461(7263), 472–475, doi:10.1038/461472a, 2009.

Roe, S.; Spivey, M.; Lindquist, H.; Thesing, K.; Strait, R.; Pechan, E.; Associates, I. Estimating Ammonia Emissions from Anthropogenic Nonagricultural Sources. EPA Emission Inventory Improvement Program. Technical Report; Emission Inventory Improvement Program, 2004.

Shephard, M.W., and Cady-Pereira, K.E.: Cross-track Infrared Sounder (CrIS) satellite observations of tropospheric ammonia, Atmos. Meas. Tech., 8, 1323-1336, 2015.

Sintermann, J., Dietrich, K., Häni, C., Bell, M., Jocher, M. and Neftel, A.: A miniDOAS instrument optimised for ammonia field measurements, Atmos. Meas. Tech., 9(6), 2721–2734, doi:10.5194/amt-9-2721-2016, 2016.

Stein, A. F., Draxler, R. R., Rolph, G. D., Stunder, B. J. B., Cohen, M. D. and Ngan, F.: NOAA's HYSPLIT Atmospheric Transport and Dispersion Modeling System, Bull. Am. Meteorol. Soc., 96(12), 2059–2077, doi:10.1175/BAMS-D-14-00110.1, 2015.

Sudesh, S, and Kulshrestha, U. C. Diurnal Variation of Ambient NH3 in Relation with Agricultural Activities and Meteorological Factors at a Rural Site in North India. Curr World Environ, SI1. DOI:http://dx.doi.org/10.12944/CWE.16.Special-Issue1.02, 2021.

Sun, K., Tao, L., Miller, D. J., Pan, D., Golston, L. M., Zondlo, M. A., Griffin, R. J., Wallace, H. W., Leong, Y. J., Yang, M. M., Zhang, Y., Mauzerall, D. L. and Zhu, T.: Vehicle Emissions as an Important Urban Ammonia Source in the United States and China, Environ. Sci. Technol., 51(4), 2472–2481, doi:10.1021/acs.est.6b02805, 2017.

Sutton, M. A., Reis, S., Riddick, S. N., Dragosits, U., Nemitz, E., Theobald, M. R., Tang, Y. S., Braban, C. F., Vieno, M., Dore, A. J., Mitchell, R. F., Wanless, S., Daunt, F., Fowler, D., Blackall, T. D., Milford, C., Flechard, C. R., Loubet, B., Massad, R., Cellier, P., Personne, E., Coheur, P. F., Clarisse, L., Van Damme, M., Ngadi, Y., Clerbaux, C., Skjøth, C. A., Geels, C., Hertel, O., Wichink Kruit, R. J., Pinder, R. W., Bash, J. O., Walker, J. T., Simpson, D., Horváth, L., Misselbrook, T. H., Bleeker, A., Dentener, F. and de Vries, W.: Towards a climate-dependent paradigm of ammonia emission and deposition, Philos. Trans. R. Soc. Lond. B. Biol. Sci., 368(1621), 20130166, doi:10.1098/rstb.2013.0166, 2013.

Sutton, M.; Dragosits, U.; Tang, Y.; Fowler, D.: Ammonia emissions from nonagricultural sources in the UK. Atmos. Environ. 34, 855– 869, DOI: 10.1016/S1352-2310(99)00362-3, 2000.

Twigg, M. M., Berkhout, A. J. C., Cowan, N., Crunaire, S., Dammers, E., Ebert, V., Gaudion, V., Haaima, M., Häni, C., John, L., Jones, M. R., Kamps, B., Kentisbeer, J., Kupper, T., Leeson, S. R., Leuenberger, D., Lüttschwager, N. O. B., Makkonen, U., Martin, N. A., Missler, D., Mounsor, D., Neftel, A., Nelson, C., Nemitz, E., Oudwater, R., Pascale, C., Petit, J.-E., Pogany, A., Redon, N., Sintermann, J., Stephens, A., Sutton, M. A., Tang, Y. S., Zijlmans, R., Braban, C. F., and Niederhauser, B.: Intercomparison of in situ measurements of ambient NH3: instrument performance and application under field conditions, Atmos. Meas. Tech., 15, 6755–6787, https://doi.org/10.5194/amt-15-6755-2022, 2022.

Van Damme, M., Clarisse, L., Stavrakou, T., Wichink Kruit, R., Sellekaerts, L., Viatte, C., Clerbaux, C. and Coheur, P.-F.: On the weekly cycle of atmospheric ammonia over European agricultural hotspots, Sci. Rep., 12(1), 12327, doi:10.1038/s41598-022-15836-w, 2022.

Van Damme, M., Clarisse, L., Franco, B., Sutton, M. A., Erisman, J. W., Wichink Kruit, R., van Zanten, M., Whitburn, S., Hadji-Lazaro, J., Hurtmans, D., Clerbaux, C., & Coheur, P.-F.: Global, regional and national trends of atmospheric ammonia derived from a decadal (2008–2018) satellite record. *Environmental Research Letters*, *16*(5), 55017. https://doi.org/10.1088/1748-9326/abd5e0, 2021.

Van Damme, M., Clarisse, L., Whitburn, S., Hadji-Lazaro, J., Hurtmans, D., Clerbaux, C. and Coheur, P.-F.: Industrial and agricultural ammonia point sources exposed, Nature, 564(7734), 99–103, doi:10.1038/s41586-018-0747-1, 2018.

Van Damme, M., Clarisse, L., Dammers, E., Liu, X., Nowak, J. B., Clerbaux, C., Flechard, C. R., Galy-Lacaux, C., Xu, W., Neuman, J. A., Tang, Y. S., Sutton, M. A., Erisman, J. W. and Coheur, P. F.: Towards validation of ammonia (NH_3) measurements from the IASI satellite, Atmos. Meas. Tech., 8(3), 1575–1591, doi:10.5194/amt-8-1575-2015, 2015.

Viatte, C. (2023). NH3 from Mini Doas [Data set]. LATMOS.

Viatte, C., Abeed, R., Yamanouchi, S., Porter, W. C., Safieddine, S., Van Damme, M., Clarisse, L., Herrera, B., Grutter, M., Coheur, P.-F., Strong, K. and Clerbaux, C.: NH_3 spatiotemporal variability over Paris, Mexico City, and Toronto, and its link to $PM_{2.5}$ during pollution events, Atmos. Chem. Phys., 22(19), 12907–12922, doi:10.5194/acp-22-12907-2022, 2022.

Viatte, C., Petit, J.-E., Yamanouchi, S., Van Damme, M., Doucerain, C., Germain-Piaulenne, E., Gros, V., Favez, O., Clarisse, L., Coheur, P.-F., Strong, K. and Clerbaux, C.: Ammonia and $PM_{2.5}$ air pollution in paris during the 2020 covid lockdown, Atmosphere, 12(2), doi:10.3390/atmos12020160, 2021.

Viatte, C., Wang, T., Van Damme, M., Dammers, E., Meleux, F., Clarisse, L., Shephard, M. W., Whitburn, S., François Coheur, P., Cady-Pereira, K. E. and Clerbaux, C.: Atmospheric ammonia variability and link with particulate matter formation: A case study over the Paris area, Atmos. Chem. Phys., 20(1), doi:10.5194/acp-20-577-2020, 2020.

Volten, H., Bergwerff, J. B., Haaima, M., Lolkema, D. E., Berkhout, A. J. C., van der Hoff, G. R., Potma, C. J. M., Wichink Kruit, R. J., van Pul, W. A. J. and Swart, D. P. J.: Two instruments based on differential optical absorption spectroscopy (DOAS) to measure accurate ammonia concentrations in the atmosphere, Atmos. Meas. Tech., 5(2), 413–427, doi:10.5194/amt-5-413-2012, 2012.

von Bobrutzki, K., Braban, C. F., Famulari, D., Jones, S. K., Blackall, T., Smith, T. E. L., Blom, M., Coe, H., Gallagher, M., Ghalaieny, M., McGillen, M. R., Percival, C. J., Whitehead, J. D., Ellis, R., Murphy, J., Mohacsi, A., Pogany, A., Junninen, H., Rantanen, S., Sutton, M. A. and Nemitz, E.: Field intercomparison of eleven atmospheric ammonia measurement techniques, Atmos. Meas. Tech., 3(1), 91–112, doi:10.5194/amt-3-91-2010, 2010.

Wang, B., Liu, Z., Li, Z., Sun, Y., Wang, C., Zhu, C., Sun, L., Yang, N., Bai, G., Fan, G., Sun, X., Xia, Z., Pan, G., Xu, C. and Yan, G.: Characteristics, chemical transformation and source apportionment of volatile organic compounds (VOCs) during wintertime at a suburban site in a provincial capital city, east China, Atmos. Environ., 298, 119621, doi:https://doi.org/10.1016/j.atmosenv.2023.119621, 2023.

Wang, S., Nan, J., Shi, C., Fu, Q., Gao, S., Wang, D., Cui, H., Saiz-Lopez, A. and Zhou, B.: Atmospheric ammonia and its impacts on regional air quality over the megacity of Shanghai, China, Sci. Rep., 5(1), 15842, doi:10.1038/srep15842, 2015.

Wang, Y.Q., Zhang, X.Y. and Draxler, R.:TrajStat: GIS-based software that uses various trajectory statistical analysis methods to identify potential sources from long-term air pollution measurement data. Environmental Modelling & Software, 24: 938-939, 2009.

Warner, J. X., Wei, Z., Strow, L. L., Dickerson, R. R., and Nowak, J. B.: The global tropospheric ammonia distribution as seen in the 13-year AIRS measurement record, Atmos. Chem. Phys., 16, 5467-5479, https://doi.org/10.5194/acp-16-5467-2016, 2016.

Wen, Y., Zhang, S., Wu, Y. and Hao, J.: Vehicular ammonia emissions: An underappreciated emission source in densely-populated areas, Atmos. Chem. Phys. Discuss., 2022, 1–14, doi:10.5194/acp-2022-828, 2022.

Whitehead, J., Longley, D., Coe, H. and Gallagher, M.: Hourly concentrations of ammonia during the winter in Manchester, UK, related to traffic and background sources, Fifth Conference on Urban Environment, Session 14 urban air quality (including urban airshed modeling and urban air chemistry experiments), Vancouver BC, Canada, 23-26 August 2004.

Zachary, M., Yin, L. and Zacharia, M.: Application of PSCF and CWT to Identify Potential Sources of Aerosol Optical Depth in ICIPE Mbita. Open Access Library Journal, 5, 1-12. doi: 10.4236/oalib.1104487, 2018.

Zhang, Q., Wei, N., Zou, C. and Mao, H.: Evaluating the ammonia emission from in-use vehicles using on-road remote sensing test, Environ. Pollut., 271, 116384, doi:https://doi.org/10.1016/j.envpol.2020.116384, 2021.